J Mol Model (2014) 20:2471
DOI 10.1007/s00894-014-2471-6

ORIGINAL PAPER

Hydration gibbs free energies of open and closed shell trivalent lanthanide and actinide cations from polarizable molecular dynamics

Aude Marjolin · Christophe Gourlaouen · Carine Clavaguéra · Pengyu Y. Ren · Jean-Philip Piquemal · Jean-Pierre Dognon

Received: 13 January 2014 / Accepted: 16 September 2014

Abstract The hydration free energies, structures, and dynamics of open- and closed-shell trivalent lanthanide and actinide metal cations are studied using molecular dynamics simulations (MD) based on a polarizable force field. Parameters for the metal cations are derived from an ab initio bottom-up strategy. MD simulations of six cations solvated in bulk water are subsequently performed with the AMOEBA polarizable force field. The calculated first-and second shell hydration numbers, water residence times, and free energies of hydration are consistent with experimental/theoretical values leading to a predictive modeling of f-elements compounds.

Keywords Hydration free energy · Lanthanides · Actinides · f-elements · Polarizable force fields

This paper belongs to Topical Collection QUITEL 2013

Electronic supplementary material The online version of this article (doi:10.1007/s00894-014-2471-6) contains supplementary material, which is available to authorized users.

A. Marjolin · J.-P. Piquemal (✉)
Laboratoire de Chimie Théorique, Sorbonne Universités, UMPC, CNRS UMR 7616, CC 137 4 Place Jussieu, 75252 Paris, Cedex 05, France
e-mail: jpp@lct.jussieu.fr

A. Marjolin · J.-P. Dognon (✉)
Laboratoire de Chimie Moléculaire et de catalyse pour l'Energie, CEA, CNRS UMR 3299, CEA Saclay, 91191 Gif-sur Yvette, Cedex, France
e-mail: jean-pierre.dognon@cea.fr

C. Gourlaouen
Laboratoire de Chimie Quantique, Université de Strasbourg, CNRS UMR 7177, PB 296 1 Rue Blaise Pascal, 67008 Strasbourg, Cedex, France

C. Clavaguéra (✉)
Laboratoire de Chimie Moléculaire, Department of Chemistry, Ecole Polytechnique, CNRS, 91 128 Palaiseau, Cedex, France
e-mail: carine.clavaguera@polytechnique.edu

P. Y. Ren
Department of Biomedical engineering, University of Texas at Austin, Austin, TX 78712-1062, USA

Introduction

Lanthanides (Ln) and Actinides (An) form the f-block of the periodic table of the elements with the progressive filling of f-orbitals across each series [1]. The two series often exhibit very similar chemical behavior, more specifically for the cations in oxidation state+III, the most common one for all the lanthanides and transplutonium actinides, namely, Am(III) and Cm(III). These cations are usually described as relatively hard acids with a strong preference for oxygen donor ligands, specifically in aqueous solution [2]. Therefore, complexation generally involves substitution of the coordinated water molecules by a ligand, which forms new metal-oxygen bonds. Even though Ln and An are said to behave quite similarly, there are still some differences that play a role in the complex formation with an organic ligand in solution [2]. During the past few years, both series have received an increasing deal of interest due to their chemical particularities and specific electronic properties [1]. However, due to the high instability of most of the 5f elements, many basic physico-chemical characteristics are still not experimentally accessible. For instance, ionization potentials or thermodynamic properties, such as hydration and binding free energies, have only been estimated by using empirical extrapolation models [3, 4]. Nevertheless, these data still remain a reference for these elements. From an atomistic simulation modeling point of view, a quantitative prediction of hydration free energy can only be accounted for by performing extensive sampling of the conformational

Published online: 09 October 2014

space using classical molecular dynamics (MD) techniques. Recent studies have shown that, in order to be predictive beyond well-described monovalent species, one needs to use a polarizable force field in order to take into account the various physical effects that contribute to the hydration properties of metal cations in solution, from divalent to tetravalent species [5–17]. Indeed, owing to high-level multipolar electrostatics and explicit treatment of polarization effects, AMOEBA force field MD simulations were able to reproduce structural and dynamical, as well as thermodynamical properties of hydrated mono and divalent metal cations [9, 10, 14, 18, 19], trivalent lanthanide cations [6–8] as well as the actinide Th(IV) cation [20].

We therefore propose a bottom-up theoretical approach to extend the AMOEBA force field to other closed-shell and open-shell trivalent lanthanide and actinide cations (La^{3+}, Eu^{3+}, Gd^{3+}, Ac^{3+}, Am^{3+} and Cm^{3+}) in order to determine the structural properties and solvation free energies of these elements, following the philosophy established recently for the Th(IV) cation [20].

Methods

Parameterization procedure

The repulsion-dispersion parameters (R and ε) of each cation M^{3+} were derived by fitting the AMOEBA van der Waals energy term on a reference ab initio potential energy surface. The diabatic interaction energy of the different $[M\text{-}OH_2]^{3+}$ systems was calculated as a function of the M-O distance at the MCSCF/MRCI level following a procedure established in our previous work [21] and as the difference between the dimer energy and those of the separate fragments.

The Stuttgart's small core quasi-relativistic effective core potential [22] and associated basis sets were used for the cation and Dunning's augmented triple zeta basis sets for H and O [23]. All calculations were carried out with the MOLPRO program package [24]. The respective active spaces, optimized cation-water distances and interaction energies are reported in Table S1 in supporting information. In addition, the damping factor "a" was adjusted so that the AMOEBA polarization energy matched the Constrained Space Orbital Variations (CSOV) [25–27] values following the procedure detailed in a previous study in which the reference ab initio polarization energy curves were presented [28].

Static electric dipole polarizabilities α of the cations were obtained by using a finite electric field perturbation method followed by a numerical differentiation of the field-dependent energies [29]. The calculations were performed at the CCSD(T) level using the MOLPRO program with the same basis sets and effective core potentials detailed above.

Molecular dynamics simulations

All MD simulations were carried out with the TINKER software package [30] at the fixed temperature of 298 K (maintained by the Berendsen thermostat [31]) with a 1 femtosecond time step, for a total simulated time of 1 nanosecond per trajectory. The Beeman algorithm [32] was used for the propagation of dynamical trajectories. Some simulations were performed on a 216 water molecule droplet in which the cations were solvated. The cluster was confined by spherical boundary conditions (SBC) with a van der Waals soft wall characterized by a 12–6 Lennard-Jones potential which was set to a fixed buffer distance of 2.5 Å outside the specified radius of 15 Å. These conditions were determined as optimal in our previous work on Th(IV) hydration [20]. Furthermore, simulations within periodic boundary condition (PBC) were also performed. The long-range electrostatics was modeled using the smooth Particle-Mesh Ewald summation [33] for atomic multipoles with a cutoff of 7 Å in real space. The convergence criterion for induced dipole computation was set to 10^{-6} D. Two boxes of different sizes were studied, one containing 215 water molecules and the cation to match the cluster conditions, and a larger box of 511 water molecules and the cation. The unit boxes have a side length of 18.643 Å and 24.857 Å respectively.

Free energy perturbation

Further MD simulations were performed to compute the solvation free energy using the Free Energy Perturbation technique. Following the procedure previously used,[14, 20] fourteen independent simulations were first performed to "grow" the van der Waals particle by first setting the charge and polarizability of the cation to zero and gradually varying R as $R(\lambda)=\lambda(R\ final)$ and ε as $\varepsilon(\lambda)=\lambda(\varepsilon\ final)$, where λ=(0.0, 0.0001, 0.001, 0.010, 0.1, 0.2, 0.3, 0.4, 0.5, 0.6, 0.7, 0.8, 0.9, 1.0). Twenty-one further simulations were then performed to "grow" the charge q of each cation along with its polarizability α such that $q(\lambda')=\lambda'(q\ final)$ and $\alpha(\lambda')=\lambda'(\alpha\ final)$, where λ′=(0.0 to 1.0 with a fixed 0.5 increment). Each simulation ran for 500 ps with a 1.0 fs time step and the same conditions as for the PBC computation of the 511 water box. The absolute free energy calculation was carried out on each of the frames saved every 0.1 ps after the first 50 ps equilibration period using the Bennet Acceptance Ratio (BAR) [34], a free energy calculation method that utilizes forward and reverse perturbations to minimize variance.

Results

The extraction of the cation parameters requires the use of accurate ab initio reference data following a recently defined

two-steps quantum chemical strategy. First, the van der Waals parameters were derived from the MCSCF/MRCI diabatic dissociation curve of the $[M(H_2O)]^{3+}$ complex. As established in reference [21], this procedure was mandatory as several avoided surface crossings occur upon M^{n+}-O dissociation, leading to charge transfer between the ion and the water molecule (e.g., S_0 curve in Fig. 1). The use of a diabatization procedure allowed us to recover the dissociation curve of the unique M^{n+}-H_2O state (S_d curve in Fig. 1) to develop polarizable ab initio-based force fields.

Second, the damping factor in the polarization energy expression [10] was adjusted on the ab initio interaction energy from a HF/MCSCF CSOV energy decomposition analysis [28]. The resulting AMOEBA parameters for the cations are provided in Table 1.

The extracted parameters were thus validated against a set of metal-water clusters of 8, 9 and 10 water molecules that are representative of the liquid phase coordination of Ln and An in water, which range from 8 to 11 in different experimental conditions. All geometries were optimized at both the MP2 and AMOEBA levels from the same starting structures. The MP2 interaction energies were calculated at the optimized geometry as the difference between the cluster energy and that of the separate fragments, and basis set superposition error corrected by the counterpoise method. The values for all ions and cluster sizes were reported in supplementary information (Table S2-S7).

The AMOEBA absolute interaction energies are in very good agreement with the MP2/cc-pVTZ ones since the global error with respect to the ab initio values is kept around 2 % (see Table S2-S7 in supporting information). Throughout the geometry optimization procedure, both the spatial organization of the water molecules around the ion (cluster symmetry and first and second shell distribution) and the energetic order of the clusters are preserved with respect to the MP2 results.

The radial distribution function (RDF) derived from MD trajectories for the different M-O_w pairs (e.g. Fig. 2 for Am^{3+}) features two well defined peaks, easily identified as the first and second hydration shells.

This shows a strong organization of the solvent around the cation. The Gaussian shape of the peak in the radial distribution function for H reflects the strong radial alignment of the water molecules under the influence of the ion. Table 2 presents the main results concerning the structure of both solvation shells around the cations in terms of coordination number and mean metal-water bond length.

A large dispersion of the experimental data on the structural parameters of the lanthanide or actinide ion hydration is observed in the literature in which the size and structure of the hydration sphere of a metal ion have been probed by direct and indirect methods. Direct methods include X-ray and neutron diffraction, X-ray absorption fine structure (XAFS) measurements, luminescence decay, and nuclear magnetic resonance (NMR) relaxation measurements, while the indirect methods involve compressibility, NMR exchange, and optical absorption spectroscopy [2]. Extended X-ray absorption fine-structure spectroscopy (EXAFS) has been widely used in the recent years in solution. EXAFS measurements are useful for determining the average ion-oxygen bond distances of the first hydration sphere with an accuracy of ca. ± 0.02 Å. But the low precision of EXAFS coordination number (reported uncertainty usually of ca. ± 20–25 %) is a well-known limitation of this technique [2, 35–38]. Another origin of the dispersion of results comes from experimental difficulties inherent to radioactive materials or arises from factors such as oxidative instability or the role of the counter-ions. For example in high-concentration solutions, the La^{3+} ion can form an inner-sphere

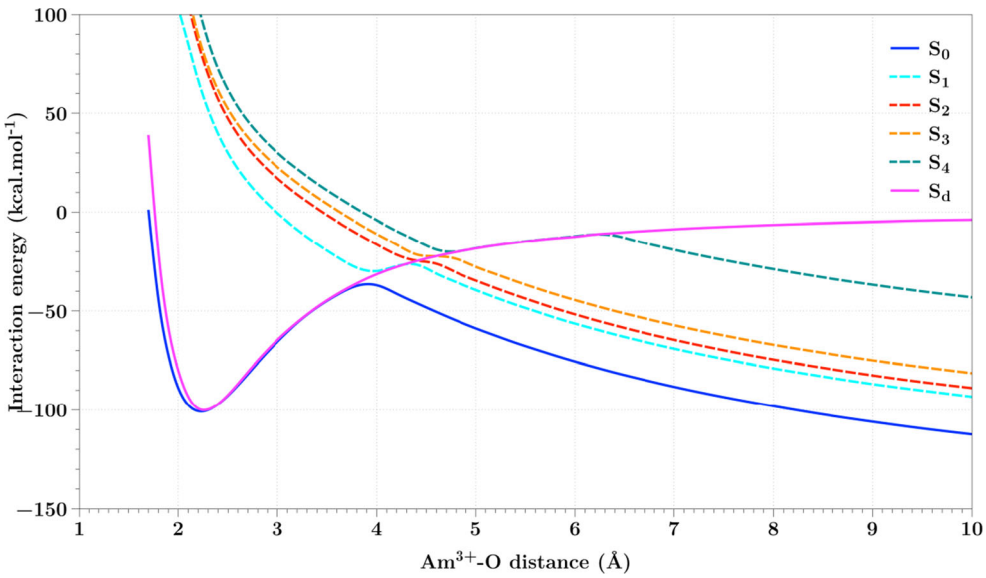

Fig. 1 Adiabatic (*blue*, *cyan*, *red*, *orange* and *green*) and diabatic (*magenta*) MRCI dissociation curves for $[Am(H_2O)]^{3+}$ complex

Table 1 Polarizabilities (α), damping factor (a), repulsion-dispersion parameters (R and ε) for each cation

Cation	α (Å^3)	a	R (Å)	ε (kcal/mol)
La(III)	1.125	0.17	3.7	3.5
Eu(III)	0.874	0.15	3.4	4.0
Gd(III)	0.836	0.15	3.3	8.5
Ac(III)	1.468	0.19	3.9	3.5
Am(III)	1.301	0.18	3.4	7.0
Cm(III)	1.147	0.18	3.4	15.0

complex with the counter-ions leading to a simultaneous loss of water molecules [39]. Recently, Smirnov and Trostin have proposed a generalization of the available literature for the Ln and An hydration based on the analysis of data in various experimental conditions [40, 41]. Their data provided in Table 2 have thus been taken as reference for the comparison with the present simulation results. The RDF profiles of all six cations are almost identical. Those results from the periodic boundary conditions (PBC) simulations on the 511 water box were found to be very similar to other smaller-scale simulations (i.e., SBC and PBC with 215 H_2O) so that the structural data are considered to be converged. However, second shell structures show a dependence on the choice of the boundary conditions and box size (Table S8 in supporting information).

For La(III), Ac(III), Am(III) and Cm(III), no water exchange was observed between the first and the second coordination shells as expected from experimental observations of the residence time of tens of ns. For cations in the middle of the Ln series (i.e. Eu(III) and Gd(III)), the CN is intermediate between 8 and 9 accounting for exchanges between the two first hydration shells. Using the notion of persistence of a water molecule [7, 42], the average residence time of a water molecule inside the first hydration shell is estimated between 0.6 and 1.0 ns in agreement with the approximate experimental value of 0.8–1.5 ns [43]. The mean metal-water bond length is also in good agreement with experiments [40, 41] since the decreasing mean bond length across each series is consistent with the decreasing ionic radii. The greater decrease of the mean bond length for Ln (La(III)/Gd(III)) in comparison with An (Ac(III)/Cm(III)) is explained by a non-negligible proportion of the 8-coordinated system with a smaller M-O_w distance for the cations in the middle of the Ln series. For the different cations, the second sphere is well resolved with a larger peak centered on a mean bond length of 4.6–4.8 Å, and an average number of water molecules matching the experimental data [40, 41, 44]. These results for the lanthanide structural data are in good agreement with the previous published ones in reference [45]. Moreover, the present AMOEBA strategy is grounded on a real global force field platform which is not limited to lanthanides and actinides and whose functional form has been extensively tried and tested to very other complex systems up to proteins. Such transferability of the AMOEBA parameters appears thus important as, despite their qualities, the other discussed framework [15] did not prove to be fully transferable; for instance it leads to a CN of 9 for Eu^{3+} and Gd^{3+} in contradiction to widely accepted intermediate value between 8 and 9, which reflects water exchanges that is observed both experimentally [43] and in our present simulations. Concerning the actinide cations, the present structural data are comparable to those obtained for the hydration of Am^{3+} and Cm^{3+} [11, 15]. No water exchange was observed between the first and the second coordination shells. For hydrated actinide cations, experimental observations are very scarce. From ^{17}O NMR spectroscopy, the residence time is ca. 185 ns for hydrated U^{4+} and superior to 20 ns for hydrated Th^{4+} [46]. The time scale on which exchange processes occur

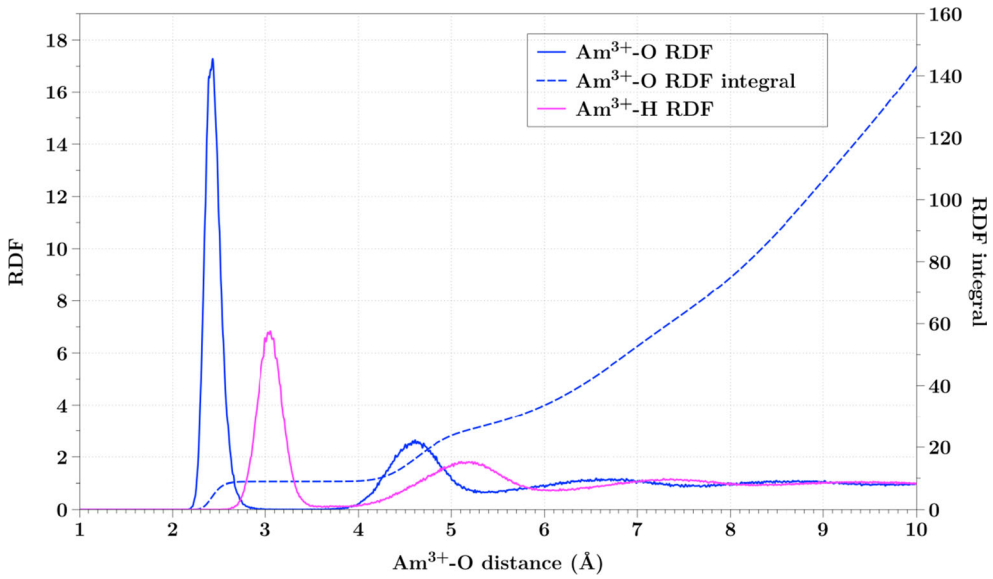

Fig. 2 Radial distribution functions (RDF) for O (and its integral) and H as a function of the Am^{3+}-O or Am^{3+}-H distance

Table 2 Coordination number (*CN*) and mean metal-water (*d*) bond length in Å from MD simulations (PBC, 511 water box) and experiments

Cation	Characteristics	511 H_2O	Experimental [40, 41]	
La(III)	1st sph.	CN	9	9
		d	2.50	2.52
	2nd sph.	CN	18	18
		d	4.69	4.65
Eu(III)	1st sph.	CN	8.8	8.8
		d	2.40	2.44
	2nd sph.	CN	15	18
		d	4.64	4.54
Gd(III)	1st sph.	CN	8.6	8.7
		d	2.38	2.42
	2nd sph.	CN	17	18
		d	4.60	4.53
Ac(III)	1st sph.	CN	9	9
		d	2.59	2.60
	2nd sph.	CN	18	N.A.
		d	4.78	N.A.
Am(III)	1st sph.	CN	9	9
		d	2.44	2.48
	2nd sph.	CN	18	N.A.
		d	4.61	N.A.
Cm(III)	1st sph.	CN	9	9
		d	2.43	2.46
	2nd sph.	CN	18	13±4
		d	4.61	4.65

is much longer than the simulation time. Due to the nature of the elements and the nature of the cation-water molecules interactions, one might expect for An(III) exchange rates several orders of magnitude larger than those obtained for Ln(III). It should be noted that the right order of magnitude of the residence time could only be obtained from classical molecular dynamics based on a polarizable force field [7]. Real et al. also investigated the Cm^{3+} hydration by polarizable force field MD simulations showing that their results strongly depend on the parameter sets [16]. For example, the organization of the two first coordination spheres around the cation behaves differently with the variation of their "charge-transfer" term. Furthermore, the CN fluctuates between 8 and 9 that implies water exchange between the two first coordination spheres which was never observed experimentally.

The Gibbs free energies of hydration for the different cations were obtained from free energy perturbation MD simulations. David et al. proposed a model [47] in order to predict and quantify thermodynamic properties of actinide aquo ions as many experimental data are missing. For a meaningful comparison, their data [3] were used as reference although some experimental data exist for lanthanides. Figure 3 reports the correlation between the resulting AMOEBA values and the reference data from David (see Table S9 in supporting information for numerical values).

The agreement found in the case of the tetravalent thorium cation from a previous study [20] was once again recovered and improved, with our computed values matching the reference data within the error bar. Furthermore, the relative ordering of the cations by increasing solvation free energy is kept. However, the difference between the hydration Gibbs energies of Eu(III) and Am(III) is strongly diminished. The deviation from reference data may arise from the lack of explicit charge transfer treatment, the absence of surface potential in the model [48]. Moreover, one should keep in mind that the reference data are derived from a mathematical model. We believe that our results are consistent and our methodology can be used for a predictive modeling of f-elements

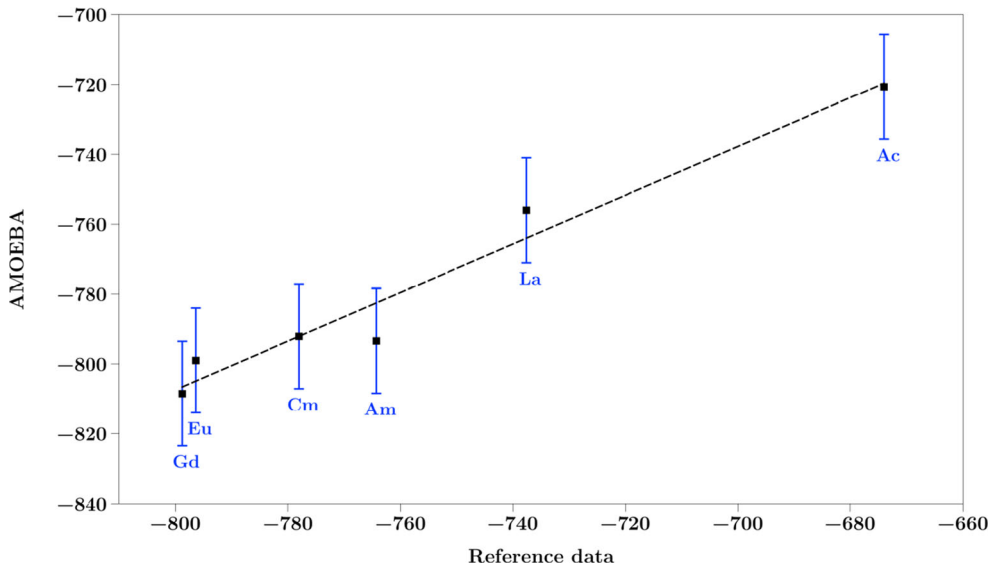

Fig. 3 Solvation free energy ΔG_{hyd} of the cations in water (kcal/mol): AMOEBA vs. reference data.[3] The calculated error bar is estimated to 15 kcal/mol. The dashed line represents the correlation (linear regression analysis) between the reference data and theoretical ΔG_{hyd}

compounds. The present results are the best available estimate of the hydration free energies of these trivalent Ln and An cations by using MD simulations based on a polarizable force field and that represent statistically the path between the initial and final states like in thermodynamics experiments.

Conclusions

Following a pioneer work on the tetravalent thorium cation [20], this successful extension of the AMOEBA polarizable force field to several closed and open shell lanthanide and actinide cations leads to conclude that the set of parameters is transferable from gas phase clusters to condensed phase. The full procedure includes the acquisition of reference ab initio data, the extraction of the parameters, the validation step on gas phase clusters, MDs yielding structural data, and finally the computation of the hydration Gibbs free energies of the cations. At each step, the results were compared to reference values, either ab initio or experimental, and showed good agreement in all cases, generally within a 2 % relative error range. Structure, energetics and thermodynamics were thus fully reproduced with respect to reference. All these conclusions will lead to future work involving the modeling of an experimental lanthanide or actinide complex in solution.

Acknowledgments P. Y. R. thanks support by the National Institute of Health (R01GM106137). A.M. thanks the CEA for a PhD grant. J.-P. D. thanks the CEA nuclear energy division DEN/RBPCH for financial support. This work was granted access to the HPC resources of [CCRT/CINES/IDRIS] under the allocation c2013086146 made by GENCI (Grand Equipement National de Calcul Intensif).

References

1. Kaltsoyannis N, Hay PJ, Li J, Blaudeau J-P, Bursten B (2011) Theoretical Studies of the Electronic Structure of Compounds of the Actinide Elements. In: Morss L, Edelstein N, Fuger J (eds) The Chemistry of the Actinide and Transactinide Elements. Springer, Netherlands, pp 1893–2012
2. Choppin G, Jensen M (2011) Actinides in Solution: Complexation and Kinetics. In: Morss L, Edelstein N, Fuger J (eds) The Chemistry of the Actinide and Transactinide Elements. Springer, Netherlands, pp 2524–2621
3. David FH (2008) About low oxidation states, hydration and covalence properties of f elements. Radiochim Acta 96(3): 135–144
4. Marcus Y (1994) A simple empirical model describing the thermodynamics of hydration of ions of widely varying charges, sizes, and shapes. Biophys Chem 51(2–3):111–127
5. Clavaguéra-Sarrio C, Brenner V, Hoyau S, Marsden CJ, Millié P, Dognon JP (2003) Modeling of uranyl cation−water clusters. J Phys Chem B 107(13):3051–3060
6. Clavaguera C, Pollet R, Soudan JM, Brenner V, Dognon JP (2005) Molecular dynamics study of the hydration of lanthanum(III) and europium(III) including many-body effects. J Phys Chem B 109(16): 7614–7616
7. Clavaguera C, Calvo F, Dognon JP (2006) Theoretical study of the hydrated Gd3+ ion: structure, dynamics, and charge transfer. J Chem Phys 124(7):74505
8. Clavaguera C, Sansot E, Calvo F, Dognon JP (2006) Gd(III) polyaminocarboxylate chelate: realistic many-body molecular dynamics simulations for molecular imaging applications. J Phys Chem B 110(26):12848–12851
9. Jiao D, King C, Grossfield A, Darden TA, Ren P (2006) Simulation of Ca2+ and Mg2+ solvation using polarizable atomic multipole potential. J Phys Chem B 110(37):18553–18559
10. Piquemal JP, Perera L, Cisneros GA, Ren P, Pedersen LG, Darden TA (2006) Towards accurate solvation dynamics of divalent cations in water using the polarizable amoeba force field: From energetics to structure. J Chem Phys 125(5):054511
11. Hagberg D, Bednarz E, Edelstein NM, Gagliardi L (2007) A quantum chemical and molecular dynamics study of the coordination of Cm(III) in water. J Am Chem Soc 129(46):14136–14137
12. Villa A, Hess B, Saint-Martin H (2009) Dynamics and structure of Ln(III)-aqua ions: a comparative molecular dynamics study using ab initio based flexible and polarizable model potentials. J Phys Chem B 113(20):7270–7281
13. Galbis E, Hernandez-Cobos J, den Auwer C, Le Naour C, Guillaumont D, Simoni E, Pappalardo RR, Sanchez Marcos E (2010) Solving the hydration structure of the heaviest actinide aqua ion known: the californium(III) case. Angew Chem Int Ed Engl 49(22):3811–3815
14. Wu JC, Piquemal JP, Chaudret R, Reinhardt P, Ren P (2010) Polarizable molecular dynamics simulation of Zn(II) in water using the AMOEBA force field. J Chem Theory Comput 6(7):2059–2070
15. D'Angelo P, Spezia R (2012) Hydration of lanthanoids(III) and actinoids(III): an experimental/theoretical saga. Chem Eur J 18(36): 11162–11178
16. Real F, Trumm M, Schimmelpfennig B, Masella M, Vallet V (2013) Further insights in the ability of classical nonadditive potentials to model actinide ion-water interactions. J Comput Chem 34(9):707–719
17. D'Angelo P, Martelli F, Spezia R, Filipponi A, Denecke MA (2013) Hydration properties and ionic radii of actinide(III) ions in aqueous solution. Inorg Chem 52(18):10318–10324
18. Grossfield A, Ren P, Ponder JW (2003) Ion solvation thermodynamics from simulation with a polarizable force field. J Am Chem Soc 125(50):15671–15682
19. Semrouni D, Isley Iii WC, Clavaguéra C, Dognon J-P, Cramer CJ, Gagliardi L (2013) Ab initio extension of the AMOEBA polarizable force field to Fe2+. J Chem Theory Comput 9(7):3062–3071
20. Marjolin A, Gourlaouen C, Clavaguéra C, Ren P, Wu J, Gresh N, Dognon J-P, Piquemal J-P (2012) Toward accurate solvation dynamics of lanthanides and actinides in water using polarizable force fields: from gas-phase energetics to hydration free energies. Theor Chem Acc 131(4):1–14
21. Gourlaouen C, Clavaguéra C, Marjolin A, Piquemal J-P, Dognon J-P (2013) Understanding the structure and electronic properties of Th4+ −water complexes. Can J Chem 91(9):821–831
22. Cao X, Dolg M, Stoll H (2003) Valence basis sets for relativistic energy-consistent small-core actinide pseudopotentials. J Chem Phys 118(2):487–496
23. Dunning JTH (1989) Gaussian basis sets for use in correlated molecular calculations. I. The atoms boron through neon and hydrogen. J Chem Phys 90(2):1007–1023
24. Werner HJ, Knowles PJ, Manby FR, Schutz M, Celani P, Knizia G, Korona T, Lindh R, Mitrushenkov A, Rauhut G, Adler TB, Amos RD, Bernhardsson A, Berning A, Cooper DL, Deegan MJO, Dobbyn AJ, Eckert F, Goll E, Hampel C, Hesselmann A, Hetzer G, Hrenar T, Jansen G, Köppl C, Liu Y, Lloyd AW, Mata RA, May AJ, McNicholas SJ, Meyer W, Mura ME, Nicklass A, Palmieri P, Pflüger K, Pitzer R, Reiher M, Shiozaki T, Stoll H, Stone AJ,

Tarroni R, Thorsteinsson T, Wang M, Wolf A (2010) MOLPRO, version 2010.1, a package of ab initio programs
25. Bagus PS, Hermann K, Bauschlicher JCW (1984) On the nature of the bonding of lone pair ligands to a transition metal. J Chem Phys 81(4):1966–1974
26. Bauschlicher JCW, Bagus PS, Nelin CJ, Roos BO (1986) The nature of the bonding in XCO for X=Fe, Ni, and Cu. J Chem Phys 85(1): 354–364
27. Piquemal JP, Marquez A, Parisel O, Giessner-Prettre C (2005) A CSOV study of the difference between HF and DFT intermolecular interaction energy values: the importance of the charge transfer contribution. J Comput Chem 26(10):1052–1062
28. Marjolin A, Gourlaouen C, Clavaguéra C, Dognon JP, Piquemal JP (2013) Towards energy decomposition analysis for open and closed shell f-elements mono aqua complexes. Chem Phys Lett 563:25–29
29. Clavaguéra C, Dognon JP (2005) Accurate static electric dipole polarizability calculations of +3 charged lanthanide ions. Chem Phys 311(1–2):169–176
30. Ponder JW (2009) TINKER: software tools for molecular design, version 6.2. 6.2 edn. Washington University School of Medicine, Saint Louis
31. Berendsen HJC, Postma JPM, van Gunsteren WF, DiNola A, Haak JR (1984) Molecular dynamics with coupling to an external bath. J Chem Phys 81(8):3684–3690
32. Beeman D (1976) Some multistep methods for use in molecular dynamics calculations. J Comput Phys 20(2):130–139
33. Essmann U, Perera L, Berkowitz ML, Darden T, Lee H, Pedersen LG (1995) A smooth particle mesh Ewald method. J Chem Phys 103(19): 8577–8593
34. Bennett CH (1976) Efficient estimation of free energy differences from Monte Carlo data. J Comput Phys 22(2):245–268
35. Allen PG, Bucher JJ, Shuh DK, Edelstein NM, Craig I (2000) Coordination chemistry of trivalent lanthanide and actinide ions in dilute and concentrated chloride solutions. Inorg Chem 39(3):595–601
36. Penner-Hahn JE (2005) Characterization of "spectroscopically quiet" metals in biology. Coord Chem Rev 249(1–2):161–177
37. Antonio M, Soderholm L (2011) X-Ray Absorption Spectroscopy of the Actinides. In: Morss L, Edelstein N, Fuger J (eds) The Chemistry of the Actinide and Transactinide Elements. Springer, Netherlands, pp 3086–3198
38. Bobyr E, Lassila JK, Wiersma-Koch HI, Fenn TD, Lee JJ, Nikolic-Hughes I, Hodgson KO, Rees DC, Hedman B, Herschlag D (2012) High-Resolution Analysis of Zn2+ Coordination in the Alkaline Phosphatase Superfamily by EXAFS and X-ray Crystallography. J Mol Biol 415(1):102–117
39. Díaz-Moreno S, Ramos S, Bowron DT (2011) Solvation structure and Ion complexation of La3+ in a 1 molal aqueous solution of lanthanum chloride. J Phys Chem A 115(24):6575–6581
40. Smirnov PR, Trostin VN (2012) Structural parameters of the nearest surrounding of lanthanide ions in aqueous solutions of their salts. Russ J Gen Chem 82(3):360–378
41. Smirnov PR, Trostin VN (2012) Sructural parameters of the nearest surrounding of tri- and tetravalent actinide ions in aqueous solutions of actinide salts. Russ J Gen Chem 82(7):1204–1213
42. Impey RW, Madden PA, McDonald IR (1983) Hydration and mobility of ions in solution. J Phys Chem 87(25):5071–5083
43. Helm L, Merbach AE (2005) Inorganic and bioinorganic solvent exchange mechanisms. Chem Rev 105(6):1923–1959
44. Skanthakumar S, Antonio MR, Wilson RE, Soderholm L (2007) The curium aqua Ion. Inorg Chem 46(9):3485–3491
45. D'Angelo P, Zitolo A, Migliorati V, Chillemi G, Duvail M, Vitorge P, Abadie S, Spezia R (2011) Revised ionic radii of lanthanoid(III) ions in aqueous solution. Inorg Chem 50(10):4572–4579
46. Farkas I, Grenthe I, Bányai I (2000) The rates and mechanisms of water exchange of actinide aqua ions: a variable temperature 17O NMR study of U(H2O)104+, UF(H2O)93+, and Th(H2O)104+. J Phys Chem A 104(6):1201–1206
47. David FH, Vokhmin V (2001) Hydration and entropy model for ionic and covalent monatomic ions. J Phys Chem A 105(42):9704–9709
48. Joung IS, Cheatham TE 3rd (2008) Determination of alkali and halide monovalent ion parameters for use in explicitly solvated biomolecular simulations. J Phys Chem B 112(30):9020–9041